THE JOURNAL OF BIOLOGICAL CHEMISTRY VOL. 288, NO. 51, pp. 36398–36408, December 20, 2013

Mitogen-activated Protein Kinase Signaling Mediates Phosphorylation of Polycomb Ortholog Cbx7*

Received for publication, May 23, 2013, and in revised form, October 28, 2013 Published, JBC Papers in Press, November 5, 2013, DOI 10.1074/jbc.M113.486266

Hsan-au Wu[‡§], Jeremy L. Balsbaugh[¶], Hollie Chandler[‖], Athena Georgilis[**], Hayley Zullow[‡], Jeffrey Shabanowitz[¶], Donald F. Hunt[¶‡‡], Jesus Gil[**], Gordon Peters[‖], and Emily Bernstein[‡§1]

*From the [‡]Department of Oncological Sciences and [§]Graduate School of Biomedical Sciences, Icahn School of Medicine at Mount Sinai, New York, New York 10029, the Departments of [¶]Chemistry and [‡‡]Pathology, University of Virginia, Charlottesville, Virginia 22904, [‖]Cancer Research UK, London Research Institute, London WC2A 3LY, United Kingdom, and the **Cell Proliferation Group, Medical Research Council Clinical Sciences Centre, Imperial College London, London W12 0NN, United Kingdom*

Background: Post-translational modification of Polycomb protein Cbx7 remains poorly understood.
Results: Here we identify and characterize a novel phosphorylation site at threonine 118 of mouse Cbx7.
Conclusion: MAPK signaling induces Cbx7 threonine 118 phosphorylation and enhances PRC1 association.
Significance: Mitogen signaling to Cbx7 confers an additional layer of PRC1 regulation.

Cbx7 is one of five mammalian orthologs of the *Drosophila* Polycomb. Cbx7 recognizes methylated lysine residues on the histone H3 tail and contributes to gene silencing in the context of the Polycomb repressive complex 1 (PRC1). However, our knowledge of Cbx7 post-translational modifications remains limited. Through combined biochemical and mass spectrometry approaches, we report a novel phosphorylation site on mouse Cbx7 at residue Thr-118 (Cbx7T118ph), near the highly conserved Polycomb box. The generation of a site-specific antibody to Cbx7T118ph demonstrates that Cbx7 is phosphorylated via MAPK signaling. Furthermore, we find Cbx7T118 phosphorylation in murine mammary carcinoma cells, which can be blocked by MEK inhibitors. Upon EGF stimulation, Cbx7 interacts robustly with other members of PRC1. To test the role of Cbx7T118 phosphorylation in gene silencing, we employed a RAS-induced senescence model system. We demonstrate that Cbx7T118 phosphorylation moderately enhances repression of its target gene p16. In summary, we have identified and characterized a novel MAPK-mediated phosphorylation site on Cbx7 and propose that mitogen signaling to the chromatin template regulates PRC1 function.

Members of the Polycomb group (PcG)[2] of proteins regulate chromatin states during development to maintain cell fate decisions (1, 2). PcG mutants, identified in *Drosophila melanogaster*, display altered body patterning caused by inappropriate Hox gene expression (3). The founding PcG member, Polycomb (Pc), is encoded by a single gene in *Drosophila*, and five Pc homologs have been identified in mammals, named Chromobox 2 (Cbx2), Cbx4, Cbx6, Cbx7, and Cbx8 (4).

Multiple PcG protein complexes exist, and two core complexes have been well characterized biochemically and functionally (5). These are the Polycomb repressive complexes 1 and 2 (PRC1 and PRC2), which contain unique histone modifying activities. PRC2 contains Ezh2 (enhancer of Zeste 2), which trimethylates H3 lysine 27 (H3K27me3), as well as other proteins such as Eed and Suz12, which are required for this activity (6–9). PRC1 complexes contain a Cbx protein that binds H3K27me3 via its conserved chromodomain (4, 10). In addition, Cbx proteins contain a conserved Pc box, required for Ring1a/b interaction within PRC1. Ring1a and Ring1b are E3 ubiquitin ligases that monoubiquitylate H2A at lysine 119 (H2AK119ub) and work cooperatively with Psc homologs, including Bmi1 and Mel-18 (11–15).

Previously, we examined the histone binding preferences of the Cbx family members and demonstrated that Cbx7, in particular, displays strong affinity for H3K27me3 and associates with facultative heterochromatin, including the inactive X chromosome (4). A functional role for Cbx7 in the context of cell cycle regulation was identified through a genetic screen that uncovered Cbx7 as a repressor of the *INK4a/ARF* locus, allowing bypass of senescence in primary human fibroblasts (16). Studies in prostate cancer and lymphoma have demonstrated its role as an oncogene (17, 18). In a developmental context, we and others have recently reported Cbx7 to be the predominant Pc protein expressed in mouse ES cells, where it acts to maintain self-renewal and pluripotency (19, 20).

Emerging evidence suggests that PcG proteins are regulated in response to the environment or cell signaling cues through post-translational modifications, particularly phosphorylation (21–24). For example, phosphorylation of Mel-18 directs Ring1b to ubiquitylate H2A in chromatin (12), and Akt-mediated EZH2 phosphorylation at serine 21 results in decreased methyltransferase activity, allowing for derepression of silenced genes (25). Collectively, phosphorylation of PcG proteins can modulate processes such as subcellular localization, protein stability,

* This work was supported, in whole or in part, by National Institutes of Health Grant GM037537 (to D. F. H.), Cancer Research UK via core funding to the London Research Institute (to G. P. and H. C.), core support from the Medical Research Council (to J. G. and A. G.), and New York State Stem Cell Science Innovative, Developmental or Exploratory Activities Award C024285 (to E. B.).

[1] To whom correspondence should be addressed: Dept. of Oncological Sciences, Icahn School of Medicine at Mount Sinai, Box 1130, New York, NY 10029. Tel.: 212-824-9335; Fax: 646-537-9576; E-mail: Emily.bernstein@mssm.edu.

[2] The abbreviations used are: Pc, Polycomb; PcG, Polycomb group; PRC, Polycomb repressive complex; Cbx, Chromobox; Cbx7T118ph, Cbx7 Thr-118 phosphorylation.

enzymatic activity, and the recruitment of other core complex components (26–30).

Although phosphorylation sites have been identified for some Pc homologs, including Cbx4, Cbx6, and Cbx8, these sites were identified by global proteomic approaches, and few functional data exist (31, 32). In this study, we report a novel phosphorylation site on Thr-118 of mouse Cbx7, which lies in close proximity to the Pc box. This site is highly conserved from *Drosophila* Pc to mammalian Cbx7, suggesting an important regulatory function. Here, we have developed a novel site-specific antibody to probe the function of Cbx7T118ph. We find that Cbx7T118ph is mediated by the MAPK pathway and is induced by serum and EGF. Furthermore, serum and EGF induced Cbx7T118ph can be blocked by MEK inhibitors. We also demonstrate MAPK-mediated Cbx7 phosphorylation in murine mammary carcinoma cells.

Functionally, we demonstrate that upon stimuli such as EGF, multiple PRC1 members are phosphorylated, and PRC1 complex association is enhanced. Using an oncogene-induced senescence model, we find that H-RAS^{V12} robustly induces Cbx7T118 phosphorylation, which in turn moderately enhances p16 repression and senescence bypass. This suggests that Cbx7T118 phosphorylation (and likely the phosphorylation of other PRC1 components) enhances the repressive ability of the PRC1. Collectively, we report a novel Cbx7 phosphorylation site and demonstrate that MAPK-mediated Cbx7T118ph regulates PRC1 function.

EXPERIMENTAL PROCEDURES

Immunoprecipitation and MS Analysis—Whole cell extracts from HEK 293 cells expressing FLAG-tagged mouse Cbx7 and parental HEK 293 cells were used for immunoprecipitation. Anti-FLAG immunoprecipitation was performed with anti-FLAG resin beads (EZView red anti-FLAG M2 affinity gel; Sigma). After immunoprecipitation, beads were washed in buffer containing 200 mM sodium chloride prior to MS analysis. For mouse ES cells expressing Cbx7-EGFP, GFP-trap beads (Chromotek) were used to precipitate GFP from ES cells expressing GFP or Cbx7-EGFP. Briefly, immunoprecipitated Cbx7 was digested and subjected to LC-MS/MS analysis using collision-activated dissociation. The methods and instrument parameters for these experiments were similar to those described previously (33, 34). MS/MS peak lists generated by Bioworks Browser (Thermo Scientific, version 3.3.1 SP1) were searched against a Cbx7 BLAST database generated from the mouse Cbx7 sequence (NCB accession number NP_659060.1) and/or a BLAST database of entire human/rat/mouse combined proteomes using the Open Mass Spectrometry Search Algorithm (version 2.1.1) (35). Cbx7 interacting specific peptide sequences and Cbx7 post-translational modifications were manually validated by visual inspection of MS/MS spectra.

Antibodies and Peptides—The following antibodies were used in the study: anti-FLAG (Sigma; F7425, F3165), anti-β-actin (Sigma; A5441), anti-Cbx7 (Millipore; 07-981), anti-β-tubulin (Millipore; 05-661), anti-Cbx7T118ph (Millipore; 06-1414), anti-H3CT-PAN (Millipore; 05-928), anti-BMI1 (Millipore; 05-1321), anti-MEL-18 (Millipore; 09-724), anti-E-cadherin (BD Biosciences; 610181), goat anti-rabbit IgG HRP (Millipore; 12-348), anti-RING1B (gift from H. Koseki; Active Motif; 39664), anti-H3S10ph (gift from C. D. Allis), anti-H3S28ph (Abcam; ab32388), anti-γH2A.X (Cell Signaling; 97185), anti-ERK (Cell Signaling; 9106), anti-ERKph (Cell Signaling; 9102), anti-Oct3/4 (BD Transduction Laboratories; 611202), and rabbit anti-mouse IgG HRP (Invitrogen; 616520). Peptide competition assays were performed as described previously (36). Phosphorylated and unphosphorylated Cbx7 peptides were made in collaboration with EMD Millipore.

Cell Culture, Plasmids, and Infections—HEK 293, murine mammary carcinoma (67NR, 168FARN, 4T07, and 4T1), and IMR90 cells were cultured in DMEM supplemented with 10% (v/v) FBS, 1% of penicillin-streptomycin. Mouse ES cells LF2 and PGK12.1 were cultured as described previously (20). Murine Cbx7 was cloned in pBabe vector with a C-terminal FLAG tag for HEK 293 cells. For mouse ES cells, murine Cbx7 was cloned in pCAGGS-L/EGFP vector as described previously (20). Thr-118 site-directed mutagenesis was carried out with a QuikChange II kit (Stratagene). Lentiviral and retroviral transductions were performed using standard procedures (37).

Cell Cycle Arrest and γ-Irradiation—Nocodazole treatment was performed as described previously (36). Cells were irradiated at 50% confluency with 10-gray dosage at the Mount Sinai Irradiator Core Facility.

Serum Starvation, Serum Induction, and EGF Stimulation—Serum induction (standard medium + 10% FBS) in HEK 293 cells began after 24 h of serum starvation (0% FBS). Recombinant human EGF stimulation (at 50 ng/ml; Peprotech; AF-100–15) in HEK 293 cells began after 24 h of serum starvation, and cells were harvested at various time points prior to 1 h.

Chromatin Fractionation and Immunoprecipitations—Chromatin fractionation was performed as described previously (4). For immunoprecipitation from the chromatin fraction, immunoprecipitation buffer (150 mM sodium chloride, 1% Nonidet P-40, 50 mM Tris, pH 7.6, and protease inhibitors from Calbiochem; 539132) was added, and the cells were sonicated (Bioruptor; Diagenode). The insoluble fraction was cleared by centrifugation prior to immunoprecipitation. After anti-FLAG immunoprecipitation, elution was performed with 3× FLAG peptide (Sigma).

Phosphatase and Kinase Assays—Lambda phosphatase (NEB P0753S) was used to treat Cbx7 FLAG eluates as per the manufacturer's instructions, and phosphatase inhibition was performed by addition of phosphatase inhibitor mixture (Millipore; 524625–1SET). Constitutive active kinases (Millipore) used are as follows: ERK1 (14-439), ERK2 (14-550), p38α/SAPK2a (14-251), JNK2α2/SAPK1a (14-329), JNK3/SAPK1b (14-501), Aurora B (14-489), CDK1/Cyclin B (14-450), and CDK2/Cyclin E (14-475). Kinase assays were performed according to the manufacturer's protocol.

Kinase Inhibitor Assays—The following kinase inhibitors were used in this study: SB203580 (Calbiochem), PD98059 (Calbiochem), U0126 (Promega), and Roscovitine (Cell Signaling). Prior to serum or recombinant human EGF induction, cells were treated with kinase inhibitor for 4 h, and the cells were harvested after 1 h of serum induction or 15 min for EGF stimulation. Kinase inhibitors were used at concentrations of

10 μM (SB203580 and U0126), 50 μM (PD98059), and 20 μM (Roscovitine).

Immunofluorescence—Immunofluorescence staining was performed as described previously (4). Cells were analyzed using the Zeiss, Axio Imager.Z1.

Immunoblot Image Analysis—Immunoblot images were quantified using ImageJ following the gel analyzer method outlined in ImageJ documentation. For each lane, PRC1 core components were normalized to total Cbx7. Cbx7 phosphorylation levels were calculated by the percentage of (area of densitometry peak from upper band)/(area of densitometry peaks of upper band and lower band) using anti-Cbx7 antibody.

Oncogene-induced Senescence—Oncogene-induced senescence was performed as described (38). Briefly, IMR90 human diploid fibroblasts were sequentially transduced with a tamoxifen-inducible H-RAS^{V12} and Cbx7 constructs. A final concentration of 10 nM 4-hydroxytamoxifen was used to induce senescence over a 2-week period. The cells were stained with crystal violet and assayed for p16 levels.

Quantitative RT-PCR Analysis—Total RNA was extracted using the RNeasy kit (Qiagen) followed by reverse transcription using SuperScript II (Invitrogen). PCRs were performed on a CFX384 real time system (Bio-Rad) using SYBR Green Master Mix (Roche Applied Science). All values were normalized to GAPDH and relative to the control using the $\Delta\Delta C_T$ method. All quantitative PCRs were performed in quadruplicate. Primers for p16 and GAPDH were as described (20, 37).

RESULTS

Identification of a Novel Cbx7 Phosphorylation Site—To investigate the post-translational modification profile of Cbx7, we performed immunoprecipitation followed by LC-MS/MS using an established HEK 293 cell line that expresses C-terminal FLAG-tagged mouse Cbx7 (Cbx7-FLAG) (4) *versus* the parental cell line as a control. Expressing mouse Cbx7 in HEK 293 cells reconstitutes a *bona fide* PRC1, because we detected core PRC1 proteins interacting with Cbx7 by MS: RING1A, RING1B, BMI1, and MEL-18, as well as less abundant components such as PHC3 and SCML2 (Fig. 1*A*) (39, 40). In addition to canonical PRC1 components, we detected additional proteins, such as the RNA helicase Mov10, as we previously described (39) (data not shown).

By probing Cbx7 immunoprecipitates, as well as whole cell extracts of Cbx7-FLAG HEK 293 cells with both Cbx7 and FLAG antibodies, we noted a distinct higher molecular weight form of Cbx7 (Fig. 1*B*). This suggested a post-translationally modified form of Cbx7. The peptides recovered from MS analysis spanned the entire Cbx7 amino acid sequence, except for the initiating methionine, and revealed a novel phosphorylation site at threonine 118 (Cbx7T118ph) (Fig. 1*C*). Further analysis by immobilized metal affinity chromatography, which enriches for phosphopeptides, validated that Thr-118 was the only phosphorylation site present at detectable levels on mouse Cbx7 (data not shown). Of note, we did not detect any human-specific CBX7 peptides in this analysis, nor did we detect human CBX7 by immunoblotting of Cbx7-FLAG immunoprecipitates with multiple Cbx7 antibodies (data not shown). This is likely due to the low level of endogenous CBX7 in HEK 293 cells (17).

The Thr-118 residue of mouse Cbx7 is highly conserved from fly to human and resides in a P*X*(S/T)P motif (Fig. 2*A*). Interestingly, a phosphorylated form of *Drosophila* Pc has been described in fly embryo extracts, but the direct site remains unknown (41). The Thr-118 residue lies in close proximity to the conserved Pc box (Fig. 2*A*), which is essential for Ring1a/b interaction (42). Intriguingly, several point mutations in this region were identified through sequencing of human tumor samples, including a proline to leucine mutation directly within the P*X*(S/T)P motif (Fig. 2*A*; data from cBioPortal for Cancer Genomics, TCGA provisional) (43, 44).

To further investigate the phosphorylation of Cbx7, we raised a mouse specific antibody against the T118ph site. Multiple assays demonstrated the specificity of the antibody, including peptide competition assays and dot blots (Fig. 2*B* and data not shown). When comparing the molecular weight of Cbx7 via immunoblotting using FLAG, Cbx7, and Cbx7T118ph antibodies, we noted that the upper band observed in the FLAG and Cbx7 blots corresponded to the band detected by the Cbx7T118ph antibody (Fig. 2*C*).

To investigate whether the mobility shift of Cbx7T118ph is due to phosphorylation, two point mutants were generated: a threonine to alanine mutant (T118A) and a threonine to glutamate mutant (T118E) to ablate and mimic phosphorylation, respectively (Fig. 2*D*). As expected, the Cbx7T118ph antibody does not recognize the mutants, and the upper band of the Cbx7 doublet is ablated in the Cbx7 T118A mutant as visualized by probing with the total Cbx7 antibody. Interestingly, the T118E mutant shows an upward shift and recapitulates the size of phosphorylated Cbx7 (Fig. 2*D*).

In addition, lambda phosphatase treatment of immunoprecipitated Cbx7 resulted in diminished Cbx7T118ph signal, which could be restored in part by the addition of phosphatase inhibitors (Fig. 2*E*). Taken together with the MS data, we conclude that the upper band of the Cbx7 doublet detected by Cbx7 and FLAG antibodies is the phosphorylated form of Cbx7 at Thr-118 and that the observed mobility shift is indeed a result of the phosphorylation charge.

Recently, we reported a role for Cbx7 as the primary Cbx family member involved in maintaining ES cell pluripotency (20). To examine Cbx7T118 phosphorylation in ES cells, we performed large scale purifications of Cbx7-EGFP from stably infected PGK12.1 cells. We were indeed able to recover two individual stretches of peptide containing the phosphorylation moiety in mouse ES cells; however, because of limited amounts of material, we could not definitively identify the phosphorylation site (Fig. 2*F*). However, using the Cbx7T118ph antibody, we were able to confirm phosphorylation in undifferentiated mouse ES cells (Fig. 2*F*). The down-regulation of Cbx7 expression is required for differentiation (19, 20), and as expected, levels of Cbx7T118ph also decrease upon differentiation (Fig. 2*F*). Of note, the Cbx7T118ph antibody appears to be mouse-specific (data not shown), and therefore the rest of our studies are focused on the murine homolog of Cbx7.

Cbx7 Thr-118 Phosphorylation Is Induced by Serum and EGF—Through the course of these studies, we noted that the levels of Cbx7T118ph varied (for example, compare Fig. 2, *D* and *E*). This suggested that Thr-118 phosphorylation might be affected

A

GI	Symbol	Protein Name	Abundance
21450179	Cbx7	chromobox 7 [*M. musculus*]	+++++
51479192	RING1A	ring finger protein 1 [*H. sapiens*]	+++
6005747	RING1B	ring finger protein 2 [*H. sapiens*]	+++
27883842	BMI1	BMI1 polycomb ring finger oncogene [*H. sapeins*]	++
6005964	MEL-18	ring finger protein 110 [*H. sapiens*]	++
148612879	PHC3	polyhomeotic like 3 [*H. sapiens*]	++
5174669	SCML2	sex comb on midleg-like 2 [*H. sapiens*]	+

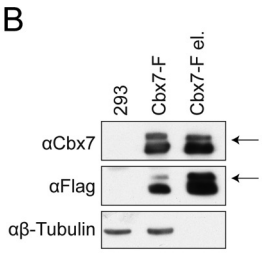

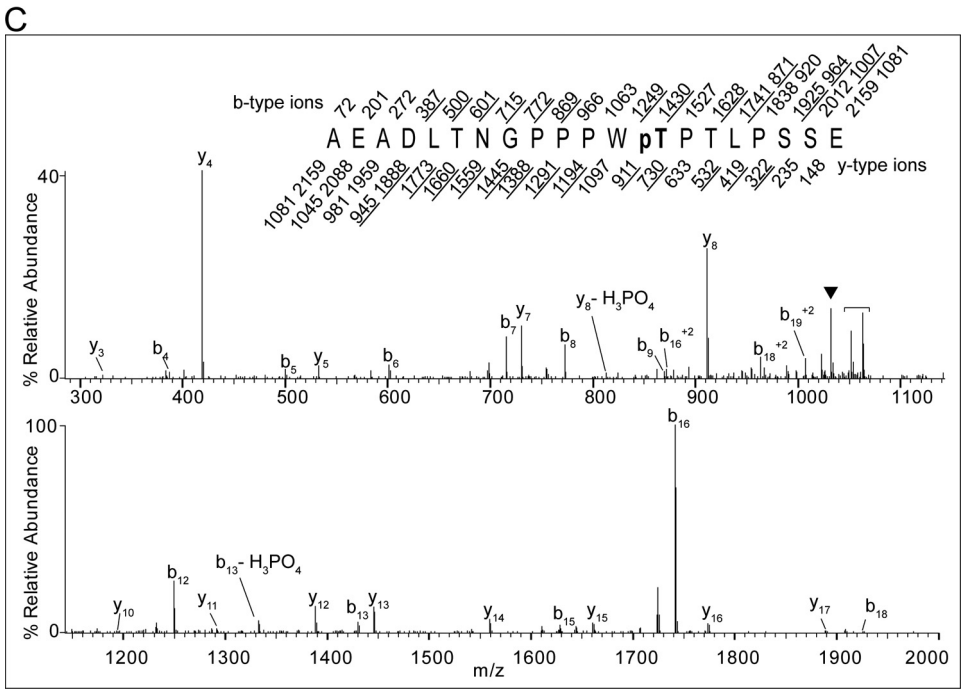

FIGURE 1. **Identification of a novel Cbx7 phosphorylation site.** *A*, abundance of Cbx7-interacting PcG-related proteins identified by MS/MS. +++++, >1000 fmol; +++, 51–100 fmol; ++, 11–50 fmol; +, 1–10 fmol. *B*, immunoblots of Cbx7 in HEK 293 parental cells; 293 Cbx7-FLAG cell whole cell extracts and FLAG eluates by FLAG and Cbx7 antibodies. β-Tubulin was used for loading. The higher molecular weight forms of Cbx7 are indicated by *arrows*. *C*, phosphorylation site mapping on Cbx7 peptide using liquid chromatography-MS/MS. The single collision-activated dissociation MS/MS spectrum was recorded on $[M + 2H]^{+2}$ ions (*m/z* 1080.90) corresponding to singly phosphorylated endoproteinase GluC-generated Cbx7 peptide, AEADLTNGPPPWpTPTLPSSE. An LTQ mass spectrometer was operated to record 10 data-dependent collision-activated dissociation MS^2 spectra after every MS^1 scan. Predicted b-type (N terminus-containing) and y-type (C terminus-containing) ions are listed above and below the peptide sequence, respectively. Singly and doubly charged fragment ions are listed as monoisotopic and average masses, respectively. Ions observed and labeled in the spectrum are *underlined* and demonstrate that the phosphate moiety is located on Thr-118. Ions corresponding to those derived from neutral losses from the precursor ion are *bracketed*. The ▼ symbol represents ions generated by the loss of the phosphate moiety from the precursor ion, $[(M + 2H) - H_3PO_4]^{+2}$.

by cell cycle events or growth conditions (*e.g.*, serum, nutrients, or growth factors). To further investigate the regulation of Cbx7T118ph, we assayed Cbx7T118ph levels in several cellular contexts.

First, we examined the phosphorylation level of Cbx7T118 during mitosis, because many PcG proteins and histones are phosphorylated upon cell division (24, 36, 45, 46). Although nocodazole-treated cells showed increased H3S10ph and H3S28ph during mitosis, Cbx7T118ph levels showed little change (Fig. 3*A*). PcG proteins and histones are also phosphorylated upon DNA damage (22, 47). Therefore, we irradiated HEK 293 cells expressing Cbx7-FLAG to induce DNA double-stranded breaks. As expected, γ-H2A.X peaked rapidly after irradiation, whereas levels of Cbx7T118ph did not change in response to DNA damage (Fig. 3*B*). Therefore, Cbx7T118 is unlikely to be phosphorylated during cell division or upon DNA damage. This is consistent with the fact that we detected ~50% of Thr-118 phosphorylation in our MS studies in asynchronous samples. Moreover, the varying levels of phosphorylation detected through the course of our studies suggested that Cbx7T118ph is likely a response to specific growth conditions.

To test this hypothesis, we examined whether Cbx7T118ph could be induced by mitogens. We first serum-starved HEK 293 cells expressing Cbx7-FLAG and then reintroduced serum and monitored Cbx7T118ph levels. Upon serum starvation, Cbx7T118ph levels were undetectable, and phosphorylation was restored within 1 h of serum reintroduction (Fig. 3*C*). The phosphorylation was sustained, at least partially, for up to 4 h after serum stimulation. We proceeded to test whether addition of recombinant human EGF could induce Cbx7T118ph levels. We found that in fact, EGF can robustly increase Cbx7T118ph levels within 15 min (Fig. 3*D*). The levels of Cbx7T118ph mirrored those of ERK phosphorylation, a readout for MAPK activity (see below), and H3S28 phosphorylation (a readout for the "nucleosomal response") was used as a positive control (48).

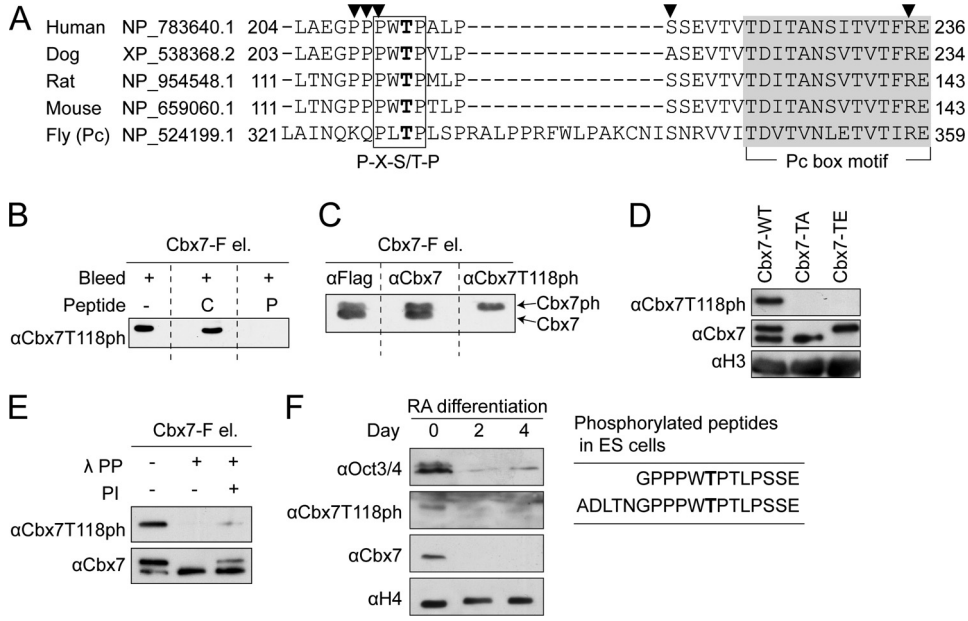

FIGURE 2. **Cbx7 is phosphorylated in a highly conserved P*X*(S/T)P motif near its Pc box.** *A*, ClustalW2 alignment of Cbx7 phosphorylation motif in different species. Cbx7T118 site is conserved across species (*bold type*). The *box* indicates the P*X*(S/T)P motif. *Shading* indicates the Pc box motif. The ▼ symbol represents putative point mutations found in human cancers (cBioPortal for Cancer Genomics, TCGA provisional). *B*, Cbx7T118ph antibody is specific as demonstrated by peptide competition assay with unphosphorylated control (*C*) and phosphorylated (*P*) peptides. *C*, immunoblot comparison of Cbx7T118ph by FLAG, Cbx7, and Cbx7T118ph antibodies. The blots were cut for incubation purposes and reassembled. *D*, chromatin fractionation of WT Cbx7 and mutants T118A (*TA*) and T118E (*TE*) probed for Cbx7 and Cbx7T118ph; histone H3 was used for loading. *E*, lambda phosphatase-treated (λ *PP*) Cbx7 FLAG eluates ± phosphatase inhibitors (*PI*); Cbx7 was used for loading. *F*, evidence of Cbx7T118ph in mouse ES cells. Two phosphorylated Cbx7 peptides were identified by MS/MS (*right*) and immunoblot of Cbx7T118ph during retinoic acid (*RA*) differentiation. Loss of Oct3/4 was used as a differentiation marker, and histone H4 was used for loading.

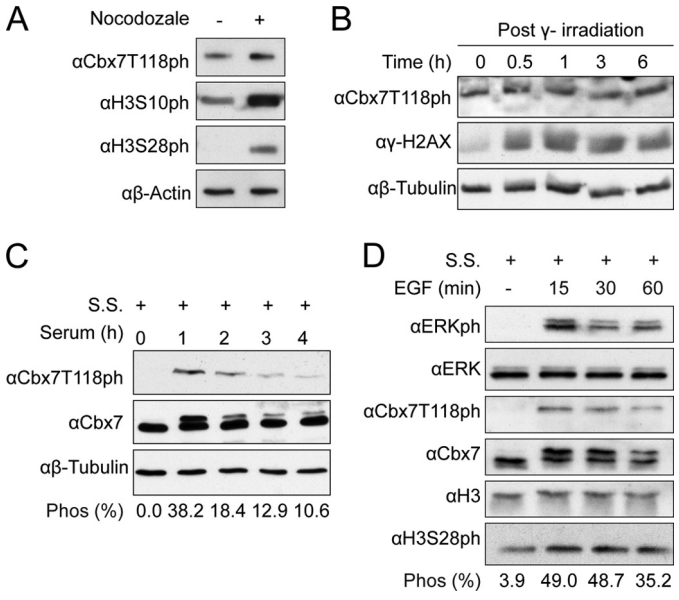

FIGURE 3. **Cbx7T118 phosphorylation is induced by serum and EGF.** *A*, immunoblot for Cbx7T118ph upon mitotic arrest by nocodazole treatment. H3S10ph and H3S28ph were used as positive controls. β-Actin was used for loading. *B*, immunoblot for Cbx7T118ph upon DNA damage induced by γ irradiation. γ-H2AX served as a positive control. β-Tubulin was used for loading. *C*, immunoblot for Cbx7T118ph upon serum starvation (*S.S.*) followed serum introduction. Histone H4 was used for loading. *D*, immunoblot for Cbx7T118ph upon EGF treatment. H3 was used for loading. The percentage of phosphorylation (*Phos*) is calculated by phosphorylated Cbx7/total Cbx7. Bands were quantified by ImageJ.

Cbx7 Thr-118 Phosphorylation Is Mediated by the MAPK Pathway—To investigate the putative kinase(s) responsible for Cbx7T118ph, we first performed *in vitro* kinase assays. Based on computational predictions of the Thr-118 phosphorylation motif (P*X*(S/T)P) (Fig. 2*A*), several candidate kinases with high prediction scores were selected, including proline-directed kinases, such as MAPKs (49). Using an unphosphorylated Cbx7 peptide containing Thr-118 as a substrate, we examined phosphorylation of the peptide using the following kinases: p44 MAPK (ERK1), p42 MAPK (ERK2), p38α MAPK (p38α), c-Jun N-terminal kinase 2 (JNK2), and JNK3. Based on our mitotic studies, Aurora B served as a negative control. Immunoblot results using the Cbx7T118ph antibody indicated that ERK1, ERK2, JNK2, and JNK3 could efficiently phosphorylate Cbx7 peptides. The stress-activated kinase p38α showed low phosphorylation efficiency for the Cbx7 peptide, similar to that of Aurora B (Fig. 4*A*). We also performed *in vitro* kinase assays with cell cycle regulators CDK1/Cyclin B (M phase) and CDK2/Cyclin E (S phase). These complexes had poor activity on the unmodified Cbx7 (data not shown). Finally, we purified Cbx7-FLAG from HEK 293 cells and upon incubation with active ERK1, and we observed efficient phosphorylation, which can be removed by lambda phosphatase treatment (Fig. 4*B*). This suggests that Cbx7 can be phosphorylated by ERK1 in the context of PRC1, at least under *in vitro* conditions.

To further examine Cbx7 Thr-118 kinase(s), HEK 293 cells were treated with kinase inhibitors in combination with serum induction. These included p38α MAPK inhibitor (SB203580), MEK inhibitors (PD98059 and U0126), and CDK inhibitor (Roscovitine). Prior to serum induction, cells were treated with respective kinase inhibitors for 4 h, and samples were subsequently collected after 1 h of serum induction. Consistent with the *in vitro* kinase assays, Cbx7T118ph was induced by serum in

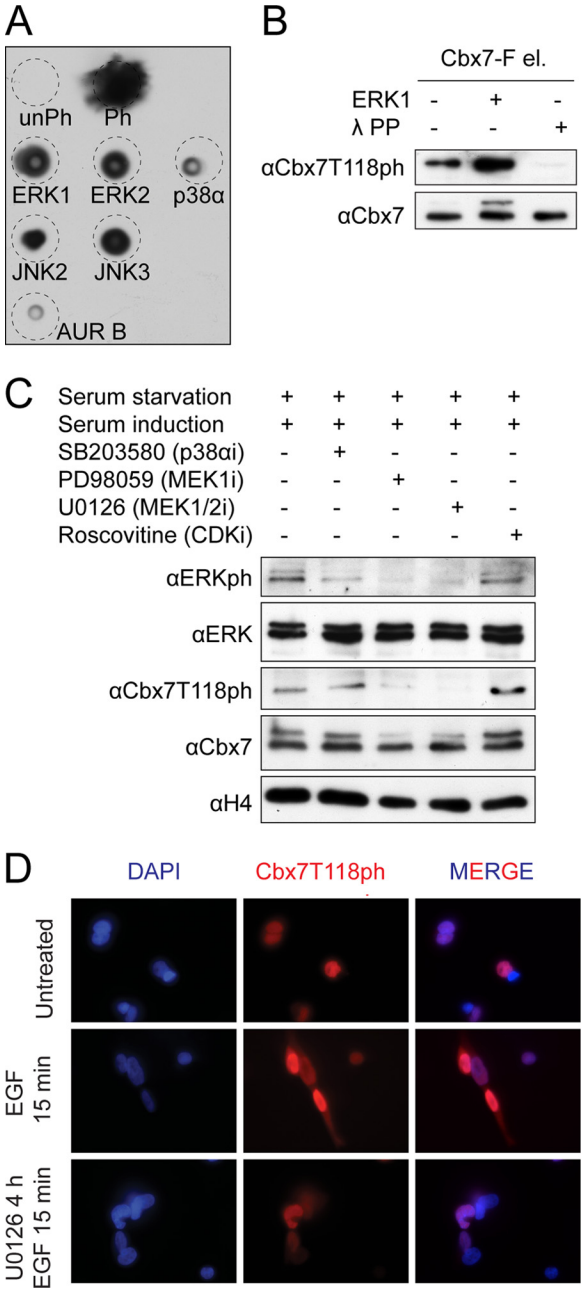

FIGURE 4. **Cbx7 Thr-118 phosphorylation is mediated by the MAPK pathway.** *A*, *in vitro* kinase assays. Unphosphorylated Cbx7 peptides were treated with ERK1, ERK2, p38α, JNK2, JNK3, and AUR B and probed for Cbx7T118ph. *unPh* represents unphosphorylated Cbx7 peptide; *Ph* represents Cbx7T118ph peptide as a positive control. *B*, *in vitro* ERK1 assays with Cbx7 FLAG eluates. Cbx7 FLAG eluates were substrates for ERK1 and lambda phosphatase (λ *PP*) and then were immunoblotted for Cbx7T118ph. *C*, HEK 293 Cbx7-FLAG cells were treated with SB230580 (p38α inhibitor), PD98059 (MEK inhibitor), and U0126 (MEK1/2 inhibitor) for 4 h prior to serum reintroduction. Cells were then harvested at 1 h after serum induction and probed for Cbx7T118ph and Cbx7. Histone H4 was used for loading. *D*, immunofluorescence of Cbx7T118ph (*red*) in HEK 293 Cbx7-FLAG cells with no treatment, stimulation with EGF for 15 min (EGF 15 min), or stimulation with EGF for 15 min combined with U1026 pretreatment for 4 h (U0126 4 h EGF 15 min). DNA was stained with DAPI (*blue*). Magnification, ×630.

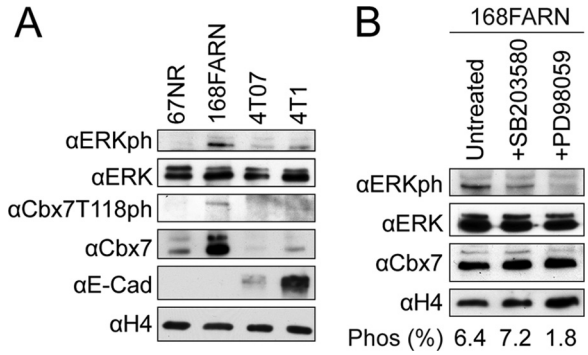

FIGURE 5. **Cbx7T118ph in mouse mammary carcinoma cells is modulated by MAPK pathway.** *A*, murine mammary carcinoma cell lines probed for Cbx7T118ph, Cbx7, ERKph, ERK, and E-cadherin. Histone H4 was used for loading. *B*, immunoblot of Cbx7T118ph in 168FARN cells treated with SB230580 or PD98059. Histone H4 was used for loading. The percentage of phosphorylation (*Phos*) is calculated by phosphorylated Cbx7/total Cbx7. Bands were quantified by ImageJ.

cells treated with SB203580 and Roscovitine, whereas inhibiting upstream of the ERK1/2 pathway was sufficient to block Cbx7T118ph, because both MEK inhibitors showed inhibitory effects on Cbx7T118ph (Fig. 4*C*). Furthermore, the addition of EGF to HEK 293 cells expressing Cbx7 showed increased Cbx7T118ph levels as detected by immunofluorescence with the site-specific antibody (Fig. 4*D*). This signal could be blocked partially by simultaneous addition of U0126 with EGF (Fig. 4*D*, *bottom row*), consistent with the data presented above. Collectively, these studies indicate that Cbx7T118ph is influenced by mitogens in serum and that recombinant EGF can induce rapid phosphorylation of Cbx7T118, both of which can be inhibited by targeting MAPK signaling via MEK.

Cbx7T118ph in Mouse Mammary Carcinoma Cells Is Modulated by MAPK Pathway—To investigate the Cbx7 phosphorylation status in tumorigenic cells, we screened isogenic mouse mammary carcinoma cell lines (67NR, 168FARN, 4T07, and 4T1) for endogenous Cbx7 and Cbx7T118ph. These cell lines have differential abilities to metastasize *in vivo*. In short, all of the cell lines can form primary tumors when implanted in the mammary fat pad; however, their metastatic potential ranges from 67NR, which does not intravasate, to 4T1 tumor cells, which are highly metastatic (50). Of the four isogenic cell lines, 168FARN cells showed the highest levels of Cbx7 and Cbx7T118ph (Fig. 5*A*).

168FARN cells have the ability to form micrometastases in lymph nodes when transplanted into the mammary fat pad; however, they do not complete all subsequent steps of metastasis (51, 52). This suggests that Cbx7 may regulate the early steps of metastasis. As expected, Cbx7T118ph levels in 168FARN coincide with the highest level of activated ERK1/2 of the four cell lines. In addition, we probed the level of the epithelial-mesenchymal transition marker E-cadherin. E-cadherin expression, which is lost during epithelial-mesenchymal transition, has been reported to be a Cbx7 target gene (53). Interestingly, we found that Cbx7 levels inversely correlated with E-cadherin, because both 67NR and 168FARN showed undetectable expression of E-cadherin (Fig. 5*A*).

Following the treatment of 168FARN cells with MEK or p38α inhibitors, we observed that only by inhibiting MEK (PD98059) could we block Cbx7 Thr-118 phosphorylation (Fig. 5*B*). These data confirm our ectopic studies of Cbx7 in HEK 293 cells and suggest that endogenous Cbx7 can be phosphorylated

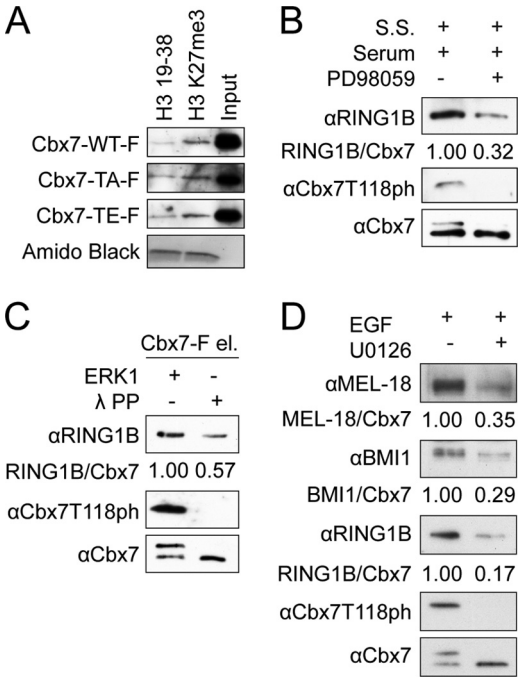

FIGURE 6. **Cbx7 Thr-118 phosphorylation regulates Cbx7-RING1B interaction.** *A*, immunoblot of wild type Cbx7, T118A, and T118E mutants in peptide pulldown assays using unmodified (H3 19–38) and H3K27me3 biotinylated peptides. Amido Black was used for loading of peptides. *B*, immunoblot of RING1B co-immunoprecipitated with FLAG-Cbx7 upon serum stimulation ± MEK inhibitor PD98059. RING1B/Cbx7 ratio was calculated using ImageJ using total Cbx7 as loading. *S.S.* = serum starvation. *C*, *in vitro* kinase-treated FLAG-Cbx7 elution with ERK1 or λ PP probed for RING1B association. *D*, immunoblot of PRC1 core components co-immunoprecipitated with FLAG-Cbx7 in chromatin. Cells were harvested 15 min after EGF stimulation ± prior treatment with MEK inhibitor U1026. Ratios were calculated using ImageJ using total Cbx7 as loading.

at Thr-118 via MAPK signaling in mouse mammary carcinoma cells.

Cbx7T118ph Regulates Interaction of PRC1 Subunits—To investigate the function of Cbx7T118 phosphorylation, we queried its ability to bind H3K27me3 through its chromodomain and potential for regulating PCR1 subunit interactions via its C-terminal Pc box. To test the former, we performed histone peptide pulldown assays with wild type Cbx7, T118A, and T118E. All three preferentially associated with H3K27me3 peptides as compared with the unmodified H3 peptides (Fig. 6*A*). This result is somewhat expected given that the chromodomain is found at the very N terminus of Cbx7. Consistent with this finding, pulldowns that we previously performed in mouse ES cells showed a doublet of Cbx7 specifically associating with the H3K27me3 peptide (20). Together, these data suggest that the phosphorylation state of Cbx7 does not alter its association with H3K27me3 (20).

Because Cbx7T118 lies in close proximity to the Pc box, we hypothesized that its phosphorylation might affect interaction with its direct binding partner Ring1b. Therefore, we stimulated cells with serum or EGF and immunoprecipitated Cbx7 to assess PRC1 components. First, we assayed RING1B association in the presence of serum with or without the addition of MEK inhibitor. As expected, upon 1 h of serum induction, we observed Cbx7T118ph, which was blocked by MEK inhibition, and here we observed a stronger association of RING1B in the immunoprecipitation of phosphorylated Cbx7 (Fig. 6*B*). This was corroborated by treatment of the purified PRC1 complex via immunoprecipitation of Cbx7-FLAG followed by on-bead *in vitro* kinase reactions. ERK1 treatment of the complex induces Cbx7T118ph, which is removed by lambda phosphatase (Fig. 6*C*). After *in vitro* treatment of PRC1 was complete, the complexes were washed extensively, and association of RING1B was assayed. As observed above, RING1B association was enhanced under phosphorylated conditions (Fig. 6*C*).

Next, we assayed PRC1 core components in the context of EGF stimulation. Upon addition of EGF (but not under MEK inhibitor treatment), immunoprecipitations showed robust association of PRC1 core components (MEL-18, BMI1, and RING1B) with Cbx7 (Fig. 6*D*). Interestingly, we also observed phosphorylation of other PRC1 subunits, besides Cbx7, such as BMI1 and MEL-18. These data suggest that EGF stimulation enhances PRC1 interactions through phosphorylation sites on multiple subunits. In fact, phosphorylation of both BMI1 and MEL-18 has previously been reported (12, 29). Therefore, we cannot exclude the possibility that phosphorylation of MEL-18, BMI1, or other PRC1 subunits contributes to PRC1 subunit association as well.

Cbx7T118ph Enhances p16 Repression in Senescence—Ectopic expression of Cbx7 can bypass the state of cellular senescence by directly suppressing the *INK4a/ARF* locus (16). Given that Cbx7T118ph is induced by MAPK signaling, we next investigated the role of Cbx7T118ph in gene silencing using an H-RAS^{V12} oncogene-induced senescence system (52). Using IMR90 cells transduced with a tamoxifen-inducible H-RAS^{V12}, we induced senescence as characterized by changes in cell morphology, decreased proliferation, and p16 up-regulation (Fig. 7*A–C*; data not shown). Transduction of Cbx7 or T118A was also performed in this system. Consistent with our findings that Cbx7T118ph is induced by the MAPK pathway, we observed a time- and dose-dependent induction of Cbx7 phosphorylation upon RAS accumulation in wild type Cbx7- but not T118A-expressing cells (Fig. 7*A*).

We next investigated whether T118ph affects the ability of Cbx7 to bypass senescence. Both wild type Cbx7 and T118A displayed senescence bypass as visualized by crystal violet staining; however, we noted a slightly less staining in the T118A-expressing cells (Fig. 7*B*). This result was supported by higher levels of p16 mRNA in the T118A mutant (Fig. 7*C*). This is particularly evident at day 14 when Cbx7 is highly phosphorylated (Fig. 7*A*). Together, these studies suggest that phosphorylation of Cbx7 T118ph is important for effective gene silencing. However, we note here that this effect is mild and may require simultaneous mutation of multiple PRC1 phosphorylation sites to achieve full derepression.

DISCUSSION

Protein phosphorylation is well recognized as an important mechanism for the regulation of cellular signaling, and a growing body of literature suggests that phosphorylation regulates chromatin dynamics (24, 45, 54). Here, we report a novel phosphorylation site on mouse Cbx7 that is highly conserved. Curiously, phosphorylation of *Drosophila* Pc in

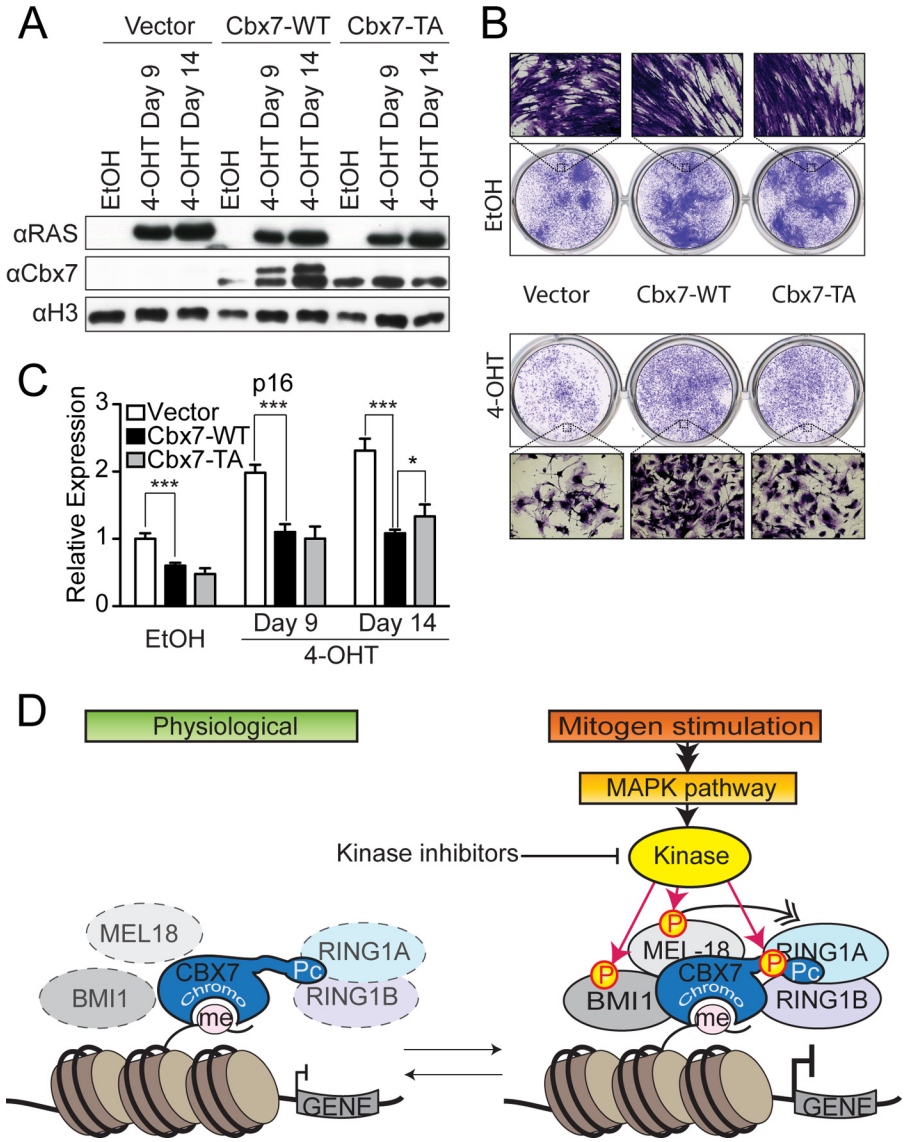

FIGURE 7. **Role of Cbx7 phosphorylation in senescence and model of MAPK pathway-mediated PRC1 regulation.** *A*, immunoblot of ectopic Cbx7 in Cbx7 WT and T118A (*TA*) transduced IMR90 ER:RAS^{V12}. Histone H3 was used for loading. *B*, crystal violet staining of cells at day 14 after selection. Magnified images (×40) show confluency and cell morphology. *C*, p16 mRNA levels measured by quantitative RT-PCR normalized to uninduced pBabe vector. ***, *p* value <0.001; *, *p* value <0.05. *D*, signaling cues induce MAPK pathway activation, which results in Cbx7T118ph, phosphorylation on MEL-18 and BMI1, and enhanced PRC1 component association. This concerted multitarget phosphorylation within PRC1 may enhance and stabilize the interaction of PRC1, in turn enhancing gene silencing.

the early fly embryo has been reported (41); however, the site has yet to be identified. Moreover, the MAPK-driven Thr-118 phosphorylation site appears specific to Cbx7 homologs, because a P*X*(S/T)P motif is not detected near the Pc box of Cbx2, Cbx4, Cbx6, or Cbx8.

Throughout the course of these studies, we noted varying levels of Cbx7 Thr-118 phosphorylation. We demonstrate that extracellular signals such as serum and EGF stimulation can rapidly phosphorylate Cbx7T118 via mitogen signaling. EGF induction has also been shown to induce rapid histone phosphorylation, namely the "nucleosomal response" (55). The phosphorylation of H3S10 and H3S28 via mitogen- and stress-activated kinases results in PcG displacement at a subset of immediate early and stress response genes by impeding Pc chromodomain binding to H3K27me3 (54, 56). However, in our study, we do not observe a global displacement of Cbx7 from chromatin upon EGF treatment (*e.g.*, Fig. 2*D* and data not shown), suggesting that the eviction of PcG proteins only occurs at a subset of PcG target genes to activate their gene expression.

Phosphorylation of BMI1 and MEL-18 has been previously reported. The kinases implicated were MK3 and PKC, respectively (28, 57). Both kinases are in the MAPK pathway and can be induced by EGF. Although we observed phosphorylation of multiple PRC1 subunits in the content of PRC1 upon EGF stimulation, we cannot definitively exclude that ERK signaling is solely responsible for our results. Our findings suggest enhanced PRC1 interactions, which is consistent with a study that showed elimination of MEL-18 phosphorylation, resulted in decreased H2A ubiquitylation levels via RING1B (12). Taken together, EGF stimulation could have two distinct outcomes at the chromatin level: one is PcG displacement by rapid histone

phosphorylation at H3S28 at a small subset of genes, and the other is global phosphorylation of PcG proteins, which enhances PRC1 interactions. The latter may be responsible for maintaining gene silencing at specific chromatin regions under such stressful conditions.

Because the antibody we generated against Cbx7T118ph recognizes the murine phosphorylation site, we focused our efforts on mouse Cbx7. However, it is interesting to note that human-derived tumor data suggest point mutations in or near the P*X*(S/T)P motif of CBX7 (Fig. 2*A*). This suggests that the Thr-118 phosphorylation motif holds important function and will be interesting to examine further in the context of cancer, particularly those tumors driven by ERK signaling, such as melanoma. To date, CBX7 has been implicated as an oncogene in prostate cancer and lymphoma, as well as a tumor suppressor in lung and breast cancer (17, 18, 58, 59). Consistent with this, we noted a loss of Cbx7 expression (and T118ph) in a series of mouse mammary carcinoma cells with increasing metastatic ability. However, we do not exclude a role for Cbx7 in tumorigenesis.

In this study, we also examined the role of Cbx7 phosphorylation in silencing a well established Cbx7 target gene, namely p16. We found that although wild type Cbx7 efficiently bypassed RAS-induced senescence and suppressed p16, Cbx7 T118A was not as effective at either (Fig. 7). Although these effects are subtle, it is not surprising that a single-site mutation is incapable of disrupting PRC1 complex function. This might require simultaneous mutation of multiple phosphorylated residues on distinct PRC1 components. At the present time, it remains unclear whether all MAPK-induced PRC1 phosphorylation sites have been characterized.

In summary, using biochemical and mass spectrometry approaches, coupled to methods that allowed us to manipulate levels of Cbx7T118ph *in vitro* and in cells, we have identified a novel phosphorylation site on Cbx7T118 and demonstrated that this phosphorylation can enhance PRC1 association upon mitogen stimulation. Our data support the notion of fine-tuning PRC1 complex interactions mediated by phosphorylation to modulate cellular processes (Fig. 7*D*). These observations contribute to a growing body of evidence suggesting that extracellular signaling can "talk" directly and rapidly to chromatin via post-translational modification of PRC1 subunits, in this case, the H3K27me3 "reader," Cbx7.

Acknowledgments—We thank the Bernstein lab members for comments and discussions on this study. We thank Ana O'Loghlen, Zulekha A. Qadeer, Kajan Ratnakumar, Alexandre Gaspar-Maia, Chi-yeh Chung, Huei-chi Wen, and Paloma Bragado for advice or critical reading of this manuscript. We thank C. David Allis (Rockefeller University), Edith Heard (Curie Institute, Paris), Stuart A. Aaronson (Mount Sinai), Julio Aguirre-Ghiso (Mount Sinai), Haruhiko Koseki (RIKEN Research Center, Yokohama City, Japan) for reagents and advice, Fred Miller (Wayne State University) for providing murine mammary carcinoma cell lines, and the antibody development scientists at EMD Millipore for collaborating on the generation of Cbx7 (catalog no. 07-981) and Cbx7T118ph (catalog no. 06-1414).

REFERENCES

1. Lewis, E. B. (1978) A gene complex controlling segmentation in *Drosophila*. *Nature* **276,** 565–570
2. Valk-Lingbeek, M. E., Bruggeman, S. W., and van Lohuizen, M. (2004) Stem cells and cancer; the polycomb connection. *Cell* **118,** 409–418
3. Beuchle, D., Struhl, G., and Müller, J. (2001) Polycomb group proteins and heritable silencing of *Drosophila* Hox genes. *Development* **128,** 993–1004
4. Bernstein, E., Duncan, E. M., Masui, O., Gil, J., Heard, E., and Allis, C. D. (2006) Mouse polycomb proteins bind differentially to methylated histone H3 and RNA and are enriched in facultative heterochromatin. *Mol. Cell. Biol.* **26,** 2560–2569
5. Whitcomb, S. J., Basu, A., Allis, C. D., and Bernstein, E. (2007) Polycomb Group proteins. An evolutionary perspective. *Trends Genet.* **23,** 494–502
6. Denisenko, O., Shnyreva, M., Suzuki, H., and Bomsztyk, K. (1998) Point mutations in the WD40 domain of Eed block its interaction with Ezh2. *Mol. Cell. Biol.* **18,** 5634–5642
7. Kuzmichev, A., Nishioka, K., Erdjument-Bromage, H., Tempst, P., and Reinberg, D. (2002) Histone methyltransferase activity associated with a human multiprotein complex containing the Enhancer of Zeste protein. *Genes Dev.* **16,** 2893–2905
8. Pasini, D., Bracken, A. P., Jensen, M. R., Lazzerini Denchi, E., and Helin, K. (2004) Suz12 is essential for mouse development and for EZH2 histone methyltransferase activity. *EMBO J.* **23,** 4061–4071
9. Müller, J., Hart, C. M., Francis, N. J., Vargas, M. L., Sengupta, A., Wild, B., Miller, E. L., O'Connor, M. B., Kingston, R. E., and Simon, J. A. (2002) Histone methyltransferase activity of a *Drosophila* Polycomb group repressor complex. *Cell* **111,** 197–208
10. Bannister, A. J., Zegerman, P., Partridge, J. F., Miska, E. A., Thomas, J. O., Allshire, R. C., and Kouzarides, T. (2001) Selective recognition of methylated lysine 9 on histone H3 by the HP1 chromo domain. *Nature* **410,** 120–124
11. de Napoles, M., Mermoud, J. E., Wakao, R., Tang, Y. A., Endoh, M., Appanah, R., Nesterova, T. B., Silva, J., Otte, A. P., Vidal, M., Koseki, H., and Brockdorff, N. (2004) Polycomb group proteins Ring1A/B link ubiquitylation of histone H2A to heritable gene silencing and X inactivation. *Dev. Cell* **7,** 663–676
12. Elderkin, S., Maertens, G. N., Endoh, M., Mallery, D. L., Morrice, N., Koseki, H., Peters, G., Brockdorff, N., and Hiom, K. (2007) A phosphorylated form of Mel-18 targets the Ring1B histone H2A ubiquitin ligase to chromatin. *Mol. Cell* **28,** 107–120
13. Wang, H., Wang, L., Erdjument-Bromage, H., Vidal, M., Tempst, P., Jones, R. S., and Zhang, Y. (2004) Role of histone H2A ubiquitination in Polycomb silencing. *Nature* **431,** 873–878
14. Cao, R., Tsukada, Y., and Zhang, Y. (2005) Role of Bmi-1 and Ring1A in H2A ubiquitylation and Hox gene silencing. *Mol. Cell* **20,** 845–854
15. Buchwald, G., van der Stoop, P., Weichenrieder, O., Perrakis, A., van Lohuizen, M., and Sixma, T. K. (2006) Structure and E3-ligase activity of the Ring-Ring complex of polycomb proteins Bmi1 and Ring1b. *EMBO J.* **25,** 2465–2474
16. Gil, J., Bernard, D., Martínez, D., and Beach, D. (2004) Polycomb CBX7 has a unifying role in cellular lifespan. *Nat. Cell Biol.* **6,** 67–72
17. Bernard, D., Martinez-Leal, J. F., Rizzo, S., Martinez, D., Hudson, D., Visakorpi, T., Peters, G., Carnero, A., Beach, D., and Gil, J. (2005) CBX7 controls the growth of normal and tumor-derived prostate cells by repressing the Ink4a/Arf locus. *Oncogene* **24,** 5543–5551
18. Scott, C. L., Gil, J., Hernando, E., Teruya-Feldstein, J., Narita, M., Martínez, D., Visakorpi, T., Mu, D., Cordon-Cardo, C., Peters, G., Beach, D., and Lowe, S. W. (2007) Role of the chromobox protein CBX7 in lymphomagenesis. *Proc. Natl. Acad. Sci. U.S.A.* **104,** 5389–5394
19. Morey, L., Pascual, G., Cozzuto, L., Roma, G., Wutz, A., Benitah, S. A., and Di Croce, L. (2012) Nonoverlapping functions of the Polycomb group Cbx family of proteins in embryonic stem cells. *Cell Stem Cell* **10,** 47–62
20. O'Loghlen, A., Muñoz-Cabello, A. M., Gaspar-Maia, A., Wu, H. A., Banito, A., Kunowska, N., Racek, T., Pemberton, H. N., Beolchi, P., Lavial, F., Masui, O., Vermeulen, M., Carroll, T., Graumann, J., Heard, E., Dillon, N., Azuara, V., Snijders, A. P., Peters, G., Bernstein, E., and Gil, J. (2012) MicroRNA regulation of Cbx7 mediates a switch of Polycomb orthologs

during ESC differentiation. *Cell Stem Cell* **10,** 33–46
21. Jacobs, J. J., Kieboom, K., Marino, S., DePinho, R. A., and van Lohuizen, M. (1999) The oncogene and Polycomb-group gene *bmi-1* regulates cell proliferation and senescence through the ink4a locus. *Nature* **397,** 164–168
22. Ginjala, V., Nacerddine, K., Kulkarni, A., Oza, J., Hill, S. J., Yao, M., Citterio, E., van Lohuizen, M., and Ganesan, S. (2011) BMI1 is recruited to DNA breaks and contributes to DNA damage-induced H2A ubiquitination and repair. *Mol. Cell. Biol.* **31,** 1972–1982
23. Ringrose, L., Rehmsmeier, M., Dura, J. M., and Paro, R. (2003) Genome-wide prediction of Polycomb/Trithorax response elements in *Drosophila melanogaster*. *Dev. Cell* **5,** 759–771
24. Niessen, H. E., Demmers, J. A., and Voncken, J. W. (2009) Talking to chromatin. Post-translational modulation of polycomb group function. *Epigenetics Chromatin* **2,** 10
25. Cha, T. L., Zhou, B. P., Xia, W., Wu, Y., Yang, C. C., Chen, C. T., Ping, B., Otte, A. P., and Hung, M. C. (2005) Akt-mediated phosphorylation of EZH2 suppresses methylation of lysine 27 in histone H3. *Science* **310,** 306–310
26. Liu, Y., Liu, F., Yu, H., Zhao, X., Sashida, G., Deblasio, A., Harr, M., She, Q. B., Chen, Z., Lin, H. K., Di Giandomenico, S., Elf, S. E., Yang, Y., Miyata, Y., Huang, G., Menendez, S., Mellinghoff, I. K., Rosen, N., Pandolfi, P. P., Hedvat, C. V., and Nimer, S. D. (2012) Akt phosphorylates the transcriptional repressor bmi1 to block its effects on the tumor-suppressing ink4a-arf locus. *Sci. Signal.* **5,** ra77
27. Tie, F., Siebold, A. P., and Harte, P. J. (2005) The N-terminus of *Drosophila* ESC mediates its phosphorylation and dimerization. *Biochem. Biophys. Res. Commun.* **332,** 622–632
28. Voncken, J. W., Niessen, H., Neufeld, B., Rennefahrt, U., Dahlmans, V., Kubben, N., Holzer, B., Ludwig, S., and Rapp, U. R. (2005) MAPKAP kinase 3pK phosphorylates and regulates chromatin association of the polycomb group protein Bmi1. *J. Biol. Chem.* **280,** 5178–5187
29. Voncken, J. W., Schweizer, D., Aagaard, L., Sattler, L., Jantsch, M. F., and van Lohuizen, M. (1999) Chromatin-association of the Polycomb group protein BMI1 is cell cycle-regulated and correlates with its phosphorylation status. *J. Cell Sci.* **112,** 4627–4639
30. Wu, S. C., and Zhang, Y. (2011) Cyclin-dependent kinase 1 (CDK1)-mediated phosphorylation of enhancer of zeste 2 (Ezh2) regulates its stability. *J. Biol. Chem.* **286,** 28511–28519
31. Roscic, A., Möller, A., Calzado, M. A., Renner, F., Wimmer, V. C., Gresko, E., Lüdi, K. S., and Schmitz, M. L. (2006) Phosphorylation-dependent control of Pc2 SUMO E3 ligase activity by its substrate protein HIPK2. *Mol. Cell* **24,** 77–89
32. Chen, R. Q., Yang, Q. K., Lu, B. W., Yi, W., Cantin, G., Chen, Y. L., Fearns, C., Yates, J. R., 3rd, and Lee, J. D. (2009) CDC25B mediates rapamycin-induced oncogenic responses in cancer cells. *Cancer Res.* **69,** 2663–2668
33. Hall, E. H., Balsbaugh, J. L., Rose, K. L., Shabanowitz, J., Hunt, D. F., and Brautigan, D. L. (2010) Comprehensive analysis of phosphorylation sites in Tensin1 reveals regulation by p38MAPK. *Mol. Cell. Proteomics* **9,** 2853–2863
34. Udeshi, N. D., Compton, P. D., Shabanowitz, J., Hunt, D. F., and Rose, K. L. (2008) Methods for analyzing peptides and proteins on a chromatographic timescale by electron-transfer dissociation mass spectrometry. *Nat. Protoc.* **3,** 1709–1717
35. Geer, L. Y., Markey, S. P., Kowalak, J. A., Wagner, L., Xu, M., Maynard, D. M., Yang, X., Shi, W., and Bryant, S. H. (2004) Open mass spectrometry search algorithm. *J. Proteome Res.* **3,** 958–964
36. Bernstein, E., Muratore-Schroeder, T. L., Diaz, R. L., Chow, J. C., Changolkar, L. N., Shabanowitz, J., Heard, E., Pehrson, J. R., Hunt, D. F., and Allis, C. D. (2008) A phosphorylated subpopulation of the histone variant macroH2A1 is excluded from the inactive X chromosome and enriched during mitosis. *Proc. Natl. Acad. Sci. U.S.A.* **105,** 1533–1538
37. Kapoor, A., Goldberg, M. S., Cumberland, L. K., Ratnakumar, K., Segura, M. F., Emanuel, P. O., Menendez, S., Vardabasso, C., Leroy, G., Vidal, C. I., Polsky, D., Osman, I., Garcia, B. A., Hernando, E., and Bernstein, E. (2010) The histone variant macroH2A suppresses melanoma progression through regulation of CDK8. *Nature* **468,** 1105–1109
38. Barradas, M., Anderton, E., Acosta, J. C., Li, S., Banito, A., Rodriguez-Niedenführ, M., Maertens, G., Banck, M., Zhou, M. M., Walsh, M. J., Peters, G., and Gil, J. (2009) Histone demethylase JMJD3 contributes to epigenetic control of INK4a/ARF by oncogenic RAS. *Genes Dev.* **23,** 1177–1182
39. El Messaoudi-Aubert, S., Nicholls, J., Maertens, G. N., Brookes, S., Bernstein, E., and Peters, G. (2010) Role for the MOV10 RNA helicase in polycomb-mediated repression of the INK4a tumor suppressor. *Nat. Struct. Mol. Biol.* **17,** 862–868
40. Shao, Z., Raible, F., Mollaaghababa, R., Guyon, J. R., Wu, C. T., Bender, W., and Kingston, R. E. (1999) Stabilization of chromatin structure by PRC1, a Polycomb complex. *Cell* **98,** 37–46
41. Poux, S., Melfi, R., and Pirrotta, V. (2001) Establishment of Polycomb silencing requires a transient interaction between PC and ESC. *Genes Dev.* **15,** 2509–2514
42. Schoorlemmer, J., Marcos-Gutiérrez, C., Were, F., Martínez, R., García, E., Satijn, D. P., Otte, A. P., and Vidal, M. (1997) Ring1A is a transcriptional repressor that interacts with the Polycomb-M33 protein and is expressed at rhombomere boundaries in the mouse hindbrain. *EMBO J.* **16,** 5930–5942
43. Cerami, E., Gao, J., Dogrusoz, U., Gross, B. E., Sumer, S. O., Aksoy, B. A., Jacobsen, A., Byrne, C. J., Heuer, M. L., Larsson, E., Antipin, Y., Reva, B., Goldberg, A. P., Sander, C., and Schultz, N. (2012) The cBio cancer genomics portal. An open platform for exploring multidimensional cancer genomics data. *Cancer Discov.* **2,** 401–404
44. Gao, J., Aksoy, B. A., Dogrusoz, U., Dresdner, G., Gross, B., Sumer, S. O., Sun, Y., Jacobsen, A., Sinha, R., Larsson, E., Cerami, E., Sander, C., and Schultz, N. (2013) Integrative analysis of complex cancer genomics and clinical profiles using the cBioPortal. *Sci. Signal.* **6,** pl1
45. Cheung, P., Allis, C. D., and Sassone-Corsi, P. (2000) Signaling to chromatin through histone modifications. *Cell* **103,** 263–271
46. Wei, Y., Yu, L., Bowen, J., Gorovsky, M. A., and Allis, C. D. (1999) Phosphorylation of histone H3 is required for proper chromosome condensation and segregation. *Cell* **97,** 99–109
47. Nacerddine, K., Beaudry, J. B., Ginjala, V., Westerman, B., Mattiroli, F., Song, J. Y., van der Poel, H., Ponz, O. B., Pritchard, C., Cornelissen-Steijger, P., Zevenhoven, J., Tanger, E., Sixma, T. K., Ganesan, S., and van Lohuizen, M. (2012) Akt-mediated phosphorylation of Bmi1 modulates its oncogenic potential, E3 ligase activity, and DNA damage repair activity in mouse prostate cancer. *J. Clin. Invest.* **122,** 1920–1932
48. Soloaga, A., Thomson, S., Wiggin, G. R., Rampersaud, N., Dyson, M. H., Hazzalin, C. A., Mahadevan, L. C., and Arthur, J. S. (2003) MSK2 and MSK1 mediate the mitogen- and stress-induced phosphorylation of histone H3 and HMG-14. *EMBO J.* **22,** 2788–2797
49. Xue, Y., Liu, Z., Cao, J., Ma, Q., Gao, X., Wang, Q., Jin, C., Zhou, Y., Wen, L., and Ren, J. (2011) GPS 2.1. Enhanced prediction of kinase-specific phosphorylation sites with an algorithm of motif length selection. *Protein Eng. Des. Sel.* **24,** 255–260
50. Aslakson, C. J., and Miller, F. R. (1992) Selective events in the metastatic process defined by analysis of the sequential dissemination of subpopulations of a mouse mammary tumor. *Cancer Res.* **52,** 1399–1405
51. Gumireddy, K., Sun, F., Klein-Szanto, A. J., Gibbins, J. M., Gimotty, P. A., Saunders, A. J., Schultz, P. G., and Huang, Q. (2007) In vivo selection for metastasis promoting genes in the mouse. *Proc. Natl. Acad. Sci. U.S.A.* **104,** 6696–6701
52. Serrano, M., Lin, A. W., McCurrach, M. E., Beach, D., and Lowe, S. W. (1997) Oncogenic ras provokes premature cell senescence associated with accumulation of p53 and p16INK4a. *Cell* **88,** 593–602
53. Federico, A., Pallante, P., Bianco, M., Ferraro, A., Esposito, F., Monti, M., Cozzolino, M., Keller, S., Fedele, M., Leone, V., Troncone, G., Chiariotti, L., Pucci, P., and Fusco, A. (2009) Chromobox protein homologue 7 protein, with decreased expression in human carcinomas, positively regulates E-cadherin expression by interacting with the histone deacetylase 2 protein. *Cancer Res.* **69,** 7079–7087
54. Gehani, S. S., Agrawal-Singh, S., Dietrich, N., Christophersen, N. S., Helin, K., and Hansen, K. (2010) Polycomb group protein displacement and gene activation through MSK-dependent H3K27me3S28 phosphorylation. *Mol. Cell* **39,** 886–900
55. Sassone-Corsi, P., Mizzen, C. A., Cheung, P., Crosio, C., Monaco, L., Jacquot, S., Hanauer, A., and Allis, C. D. (1999) Requirement of Rsk-2 for

epidermal growth factor-activated phosphorylation of histone H3. *Science* **285,** 886–891

56. Lau, P. N., and Cheung, P. (2011) Histone code pathway involving H3 S28 phosphorylation and K27 acetylation activates transcription and antagonizes polycomb silencing. *Proc. Natl. Acad. Sci. U.S.A.* **108,** 2801–2806
57. Fujisaki, S., Ninomiya, Y., Ishihara, H., Miyazaki, M., Kanno, R., Asahara, T., and Kanno, M. (2003) Dimerization of the Polycomb-group protein Mel-18 is regulated by PKC phosphorylation. *Biochem. Biophys. Res. Commun.* **300,** 135–140
58. Forzati, F., Federico, A., Pallante, P., Abbate, A., Esposito, F., Malapelle, U., Sepe, R., Palma, G., Troncone, G., Scarfò, M., Arra, C., Fedele, M., and Fusco, A. (2012) CBX7 is a tumor suppressor in mice and humans. *J. Clin. Invest.* **122,** 612–623
59. Zhang, X. W., Zhang, L., Qin, W., Yao, X. H., Zheng, L. Z., Liu, X., Li, J., and Guo, W. J. (2010) Oncogenic role of the chromobox protein CBX7 in gastric cancer. *J. Exp. Clin. Cancer Res.* **29,** 114